

# The influence of magnetic sublattice dilution on magnetic order in $\text{CeNiGe}_3$ and $\text{UNiSi}_2$

A P Pikul

Institute of Low Temperature and Structure Research, Polish Academy of Sciences,  
P Nr 1410, 50–590 Wrocław 2, Poland

E-mail: A.Pikul@int.pan.wroc.pl

**Abstract.** Polycrystalline samples of the Y-diluted antiferromagnet  $\text{CeNiGe}_3$  ( $T_N = 5.5$  K) and Th-diluted ferromagnet  $\text{UNiSi}_2$  ( $T_C = 95$  K) were studied by means of x-ray powder diffraction, magnetization and specific heat measurements performed in a wide temperature range. The lattice parameters of the  $\text{Ce}_{1-x}\text{Y}_x\text{NiGe}_3$  alloys decrease linearly with increasing the Y content, while the unit cell volume of  $\text{U}_{1-x}\text{Th}_x\text{NiSi}_2$  increases linearly with rising the Th content. The ordering temperatures of the systems decrease monotonically with increasing  $x$  down to about 1.2 K in  $\text{Ce}_{0.4}\text{Y}_{0.6}\text{NiGe}_3$  and 26 K in  $\text{U}_{0.3}\text{Th}_{0.7}\text{NiSi}_2$ , forming a dome of a long-range magnetic order on their magnetic phase diagrams. The suppression of the magnetic order is associated with distinct broadening of the anomalies at  $T_{N,C}$  due to crystallographic disorder being a consequence of the alloying. Below the magnetic percolation threshold  $x_c$  of about 0.68 and 0.75 in the Ce- and U-based alloys, respectively, the long-range magnetic order smoothly evolves into a short-range one, forming a tail on the magnetic phase diagrams. The observed behaviour  $\text{Ce}_{1-x}\text{Y}_x\text{NiGe}_3$  and  $\text{U}_{1-x}\text{Th}_x\text{NiSi}_2$  is characteristic of diluted magnetic alloys.

Submitted to: *J. Phys.: Condens. Matter*

## 1. Introduction

Partial substitution of some chemical elements by another ones, is one of the methods of modifying and examining the ground states of intermetallic compounds with unique physical properties. Such alloying (or doping) is particularly fruitful in strongly correlated electron systems, in which different sizes and electron configurations of the swapped atoms may significantly influence the exchange integral, being one of the crucial parameters determining magnetic properties of these systems [1, 2, 3]. Additionally, the chemical doping introduce some structural disorder, which can be another source of non-trivial magnetic behaviour [4].

In the course of our studies of the influence of the chemical substitution on physical properties of selected dense Kondo systems [5, 6, 7, 8, 9, 10], we have performed alloying studies of two ternary intermetallic phases, namely  $\text{CeNiGe}_3$  and  $\text{UNiSi}_2$ , crystallizing

in two orthorhombic and – to some extent – similar structures of the SmNiGe<sub>3</sub>- [11] and CeNiSi<sub>2</sub>-type [12], respectively. CeNiGe<sub>3</sub> orders antiferromagnetically below the Néel temperature  $T_N = 5.5$  K and exhibits features of a dense Kondo system with the Kondo temperature  $T_K$  being close to  $T_N$  [13]. Physical properties measurements performed under hydrostatic pressure revealed that the Néel temperature of CeNiGe<sub>3</sub> initially increases with increasing pressure up to about 8 K at  $P_{\max} \approx 3$  GPa. At higher pressure  $T_N$  rapidly decreases and the antiferromagnetic order is suppressed at the critical pressure  $P_c = 5.5$  GPa. Simultaneously, the 4*f*-electrons of cerium become partly delocalized and at about 8 GPa the compound exhibits features of an intermediate valence system. Most importantly, at the critical pressure CeNiGe<sub>3</sub> becomes superconducting below  $T_c = 0.48$  K [14, 15] and – as revealed by nuclear quadrupole resonance measurements – the superconductivity has an unconventional character resulting from the presence of the 4*f* electrons of cerium [16, 17, 18]. Interestingly, also in YNiGe<sub>3</sub>, being an isostructural non-*f*-electron reference to CeNiGe<sub>3</sub>, a superconducting phase transition was found below about 0.48 K, yet at ambient pressure [19]. UNiSi<sub>2</sub> exhibits in turn a ferromagnetic order of nearly localized magnetic moments of uranium ( $T_C = 95$  K) and some features characteristic of Kondo lattices [20, 10]. Our investigations of the solid solutions UNi<sub>1-x</sub>Co<sub>x</sub>Si<sub>2</sub> ( $0 \leq x \leq 1$ ) indicated a very robust nature of the ferromagnetism observed in the parent compound UNiSi<sub>2</sub> – although the ferromagnetic ordering is gradually suppressed upon stepwise substitution of Ni by Co, the phase transition exhibits clearly the ferromagnetic character up to  $x = 0.96$  [21]. Recent pressure experiments performed on UNiSi<sub>2</sub> showed that the ferromagnetism of the compound is quenched above 5.5 GPa, where the 5*f*-electrons of uranium become delocalized [22].

In order to shed more light on the intriguing properties of CeNiGe<sub>3</sub> and UNiSi<sub>2</sub> we have investigated physical properties of their solid solutions with their non-magnetic isostructural counterparts YNiGe<sub>3</sub> and ThNiSi<sub>2</sub>, respectively. Please note, that LaNiGe<sub>3</sub>, which would be a more appropriate reference for CeNiGe<sub>3</sub>, most probably does not exist [13]. In this paper we present results of the magnetic susceptibility and specific heat measurements, indicating suppression of the long-range magnetic order and its smooth evolution into a short-range one.

## **2. Experimental details**

Polycrystalline samples of the alloys Ce<sub>1-x</sub>Y<sub>x</sub>NiGe<sub>3</sub> and U<sub>1-x</sub>Th<sub>x</sub>NiSi<sub>2</sub> ( $0 \leq x \leq 1$ ) were prepared by conventional arc melting the stoichiometric amounts of the elemental components in protective atmosphere of an argon glove box. The pellets with Ce were subsequently wrapped in a molybdenum foil, sealed in an evacuated silica tube, and annealed at 800°C for one week, while the U-based samples were wrapped in a tantalum foil annealed for four weeks. The quality of the products was checked by means of x-ray powder diffraction, which showed that all the samples were single phases.

Magnetic properties of the alloys were studied using a commercial Quantum Design

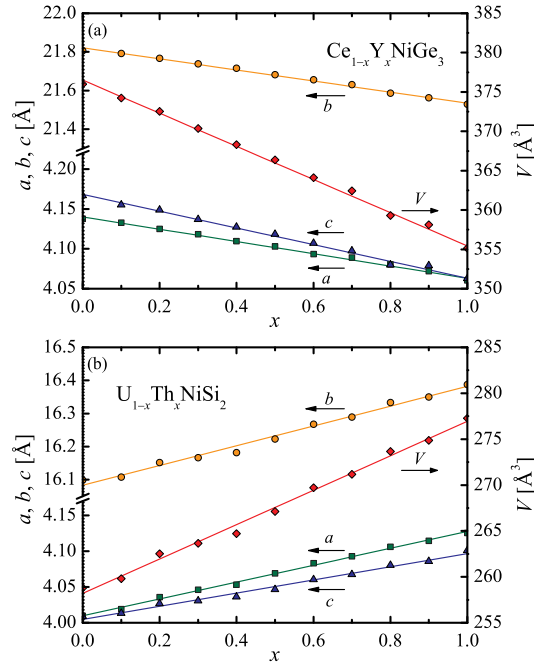


**Figure 1.** Lattice parameters  $a$ ,  $b$  and  $c$  and unit cell volume  $V$  of the  $\text{Ce}_{1-x}\text{Y}_x\text{NiGe}_3$  (a) and  $\text{U}_{1-x}\text{Th}_x\text{NiSi}_2$  (b) alloys as a function of the nominal yttrium and thorium contents  $x$ , respectively. Solid lines represent linear fits to the experimental data.

Magnetic Property Measurement System at temperatures 1.7–400 K and in magnetic fields up to 5 T. The heat capacity was measured at temperatures ranging from 360 mK up to room temperature, using a Quantum Design Physical Property Measurement System.

### 3. Results

#### 3.1. Crystal structure

Analysis of the x-ray powder diffraction patterns (not presented here) confirmed that  $\text{CeNiGe}_3$  and  $\text{YNiGe}_3$  crystallize in the  $\text{SmNiGe}_3$ -type structure (space group  $Cmmm$  [11]), while  $\text{UNiSi}_2$  and  $\text{ThNiSi}_2$  – in the  $\text{CeNiGe}_2$ -type structure (space group  $Cmcm$  [12]). The refined lattice parameters are  $a = 4.1377(5)$  Å,  $b = 21.807(3)$  Å and  $c = 4.1668(5)$  Å for  $\text{CeNiGe}_3$ ,  $a = 4.0604(5)$  Å,  $b = 21.529(2)$  Å and  $c = 4.0627(3)$  Å for  $\text{YNiGe}_3$ ,  $a = 4.0097(5)$  Å,  $b = 16.099(2)$  Å, and  $c = 4.0089(5)$  Å for  $\text{UNiSi}_2$ , and  $a = 4.1256(4)$  Å,  $b = 16.388(2)$  Å, and  $c = 4.1009(5)$  Å for  $\text{ThNiSi}_2$ , all being close to the values reported in the literature [11, 12, 23, 20]. The Rietveld refinement revealed that partial substitution of Ce by smaller Y and U by larger Th does not change the crystal structures of the systems but results – respectively – in linear compression and expansion of the lattice. As can be inferred from figure 1, the observed change of the unit-cell volume (in total up to -6% in the Ce phases and +7% in the U alloys) is in both systems monotonic and linear in  $x$  in each principal crystallographic direction.

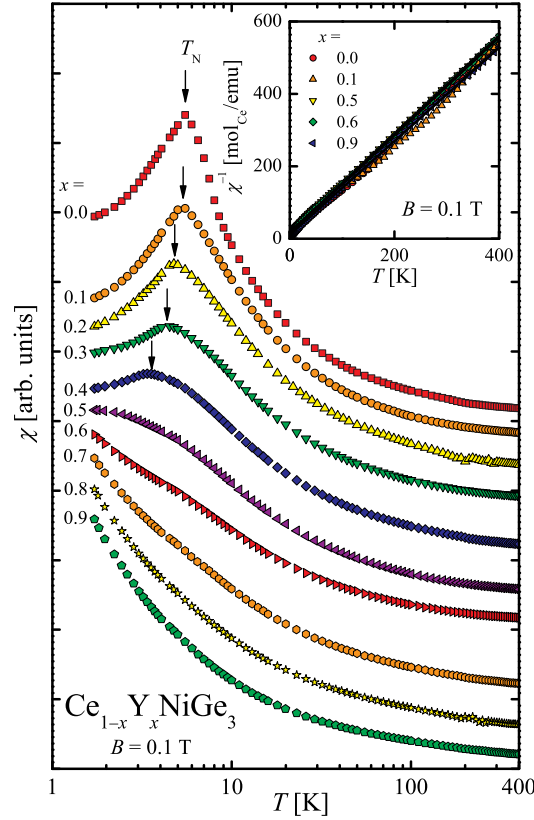


**Figure 2.** Temperature variations of the magnetic susceptibility  $\chi$  of  $\text{Ce}_{1-x}\text{Y}_x\text{NiGe}_3$  in a logarithmic scale. The curves are shifted upward for the sake of clarity; the arrows mark the antiferromagnetic phase transition temperatures  $T_N$ . Inset:  $\chi^{-1}$  vs.  $T$  for selected compositions. Straight solid lines represent the Curie-Weiss fits.

### 3.2. Magnetic properties

The magnetic susceptibility measurements performed for the parent compounds  $\text{CeNiGe}_3$  and  $\text{YNiGe}_3$  confirmed the previous findings [13, 14, 24]. In particular,  $\text{CeNiGe}_3$  exhibits localised antiferromagnetism below 5.5 K, while  $\text{YNiGe}_3$  is an itinerant paramagnet with nearly temperature independent magnetic susceptibility  $\chi(T)$  (not shown here). Figure 2 displays  $\chi(T)$  of  $\text{Ce}_{1-x}\text{Y}_x\text{NiGe}_3$ . As is apparent from the inset to Fig. 2, the  $\chi^{-1}(T)$  curves exhibit linear behavior above about 100 K and – as normalised per mole of Ce atoms – are nearly superimposed onto each other. Least square fits of the Curie-Weiss law (i.e.  $\chi(T) = (1/8)\mu_{\text{eff}}^2/(T - \theta_p)$ ) to the experimental data (see the solid lines in the inset to Fig. 2) yielded for each alloy the effective magnetic moment  $\mu_{\text{eff}}$  of about  $2.5(1) \mu_B$  and the paramagnetic Curie temperature  $\theta_p$  ranging between  $-20(5)$  and  $-10(5)$  K. The values of  $\mu_{\text{eff}}$  are close to the theoretical Hund’s-rules magnetic moment calculated for a free  $\text{Ce}^{3+}$  ion (i.e.  $2.54 \mu_B$ ), pointing to the presence of well localized cerium magnetic moments in all the alloys studied. The negative  $\theta_p$  values are in line with antiferromagnetic exchange interactions, and their relatively large absolute values (in comparison to  $T_N$ ) suggest the presence of the Kondo interactions in the

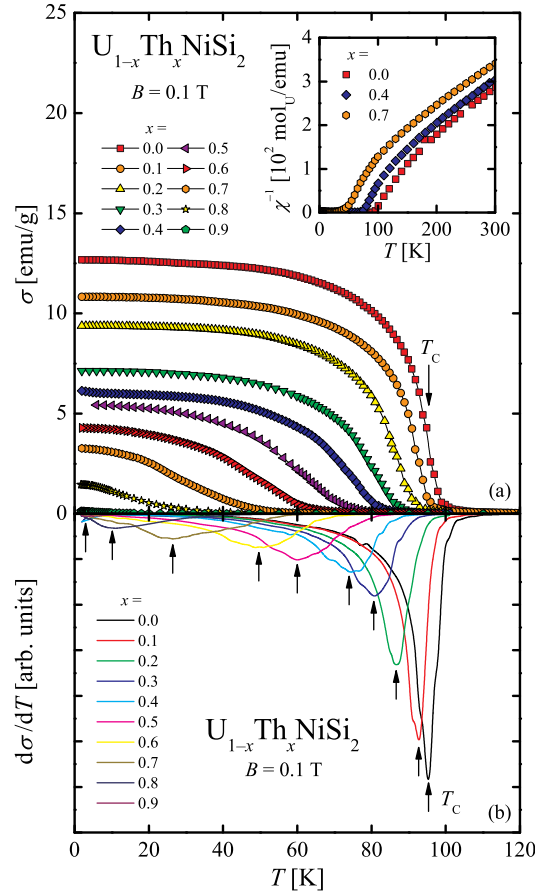


**Figure 3.** (a) Magnetization  $\sigma$  of  $\text{U}_{1-x}\text{Th}_x\text{NiSi}_2$  as a function of temperature  $T$  measured in constant magnetic field  $B$  in a field-cooling regime; the arrow marks the ferromagnetic ordering temperature  $T_C$ . Inset:  $\chi^{-1}$  vs.  $T$  for selected compositions. (b) Temperature derivative of  $\sigma(T)$ ; the arrows mark the ordering temperatures.

alloys. Due to significant scatter in the  $\theta_p$  values (not shown here), no clear evolution was found in the  $\theta_p(x)$  dependence. The deviation of  $\chi^{-1}(T)$  from the linear behavior below 100 K can be ascribed to thermal depopulation of the crystalline electric field levels of the cerium ions. Upon increasing  $x$ , the cusp visible in  $\chi(T)$  of  $\text{Ce}_{1-x}\text{Y}_x\text{NiGe}_3$  at  $T_N$  moves towards lower temperatures and significantly broadens. For  $x = 0.50$  the maximum is hardly visible in the magnetic susceptibility above 2 K (Fig. 2).

Figure 3 presents the magnetic properties of the  $\text{U}_{1-x}\text{Th}_x\text{NiSi}_2$  alloys.  $\text{UNiSi}_2$  orders ferromagnetically at the Curie temperature  $T_C = 95$  K (as reported earlier [20]), while its isostructural non- $f$ -electron reference compound  $\text{ThNiSi}_2$  is a weak Pauli-like paramagnet. At elevated temperatures, the  $\chi^{-1}(T)$  curves appeared to have similar shape and to be nearly parallel to each other (see the inset to Fig. 3). Such a behaviour suggests that the effective magnetic moment of uranium does not change significantly upon increasing  $x$ , yet its exact value can not be estimated from the Curie–Weiss fits (due to partial delocalization of the  $5f$  electrons and the crystalline electric field splitting exceeding the temperature range studied). As apparent in figure 3(a), the

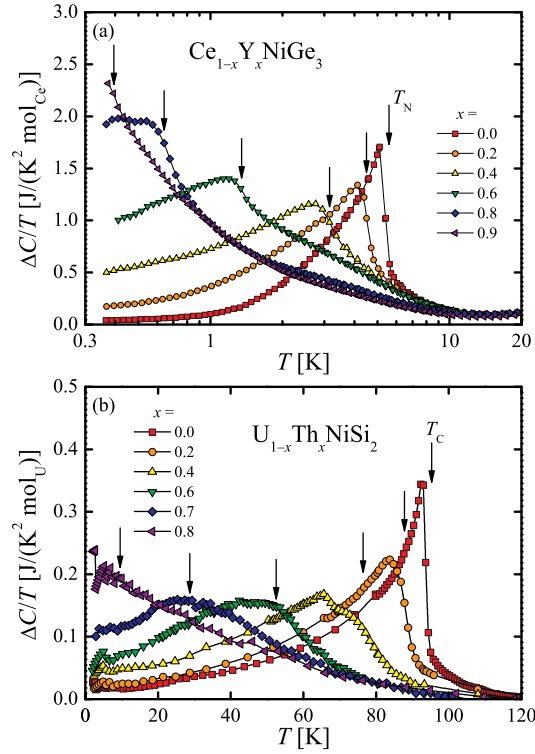


**Figure 4.** Temperature dependence of a non-phononic contribution  $\Delta C$  to the total specific heat of selected  $\text{Ce}_{1-x}\text{Y}_x\text{NiGe}_3$  (a) and  $\text{U}_{1-x}\text{Th}_x\text{NiSi}_2$  (b) alloys, normalized per mole of cerium or uranium, respectively, and divided by  $T$ . The solid lines serve as guides for the eye and the arrows mark the phase transition temperatures from temperature derivatives of  $\Delta C(T)/T$ .

initial Brillouin-shaped  $\sigma(T)$  curve significantly broadens and flattens upon diluting the magnetic sublattice and  $T_C$  defined as a position of the minimum in temperature derivative of  $\sigma(T)$  (figure 3(b)) decreases monotonically with increasing  $x$ .

### 3.3. Thermodynamic properties

Figure 4(a) displays the low temperature variation of the  $4f$ -electron contribution  $\Delta C$  to the total specific heat of  $\text{Ce}_{1-x}\text{Y}_x\text{NiGe}_3$ , estimated by subtracting the phonon specific heat of  $\text{YNiGe}_3$  (cf. [13]), normalized per mole of cerium and divided by  $T$ . As seen, the antiferromagnetic ordering of  $\text{CeNiGe}_3$  at  $T_N = 5.5$  K manifests itself as a distinct  $\lambda$ -shaped anomaly in  $\Delta C(T)/T$ , being in agreement with the previous reports [13, 25]. Upon diluting the Ce-sublattice with Y, the phase transition anomaly significantly broadens and its position (here defined as a minimum in the second derivative of  $\Delta C(T)/T$ ; not presented here) moves to 1.35 K for  $x = 0.6$ . Finally, in the most diluted alloy studied, i.e.  $\text{Ce}_{0.1}\text{Y}_{0.9}\text{NiGe}_3$ , only a very weak signature of the phase transition can be found in temperature derivative of  $\Delta C(T)/T$  at about 0.39 K.

Similar behaviour has been found in the temperature dependence of the  $5f$ -electron contribution to the specific heat of  $\text{U}_{1-x}\text{Th}_x\text{NiSi}_2$ , obtained by subtracting the phonon

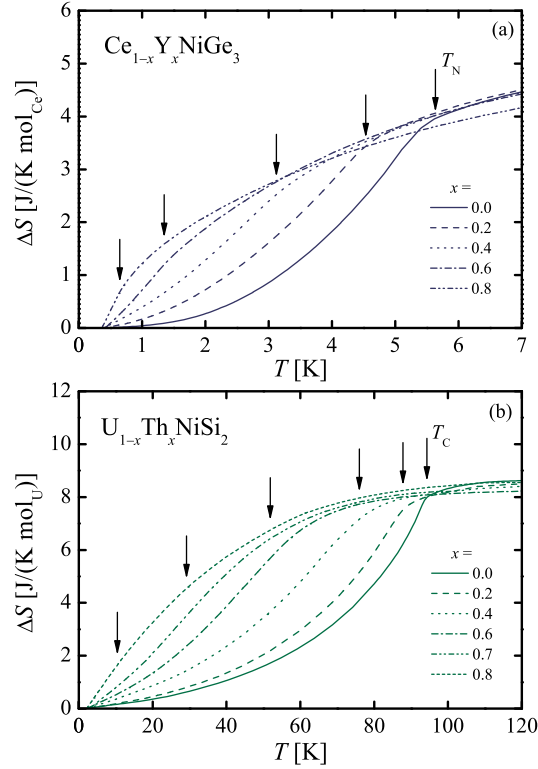


**Figure 5.** Increase of magnetic entropy  $\Delta S$  of selected  $\text{Ce}_{1-x}\text{Y}_x\text{NiGe}_3$  (a) and  $\text{U}_{1-x}\text{Th}_x\text{NiSi}_2$  (b) alloys as a function of temperature  $T$ . The arrows mark the Néel ( $T_N$ ) and Curie ( $T_C$ ) temperatures from  $\Delta C(T)/T$  (figure 4).

contribution of  $\text{ThNiSi}_2$  (figure 4(b)). In particular, the distinct  $\lambda$ -shaped anomaly in  $\Delta C(T)/T$  manifests the ferromagnetic ordering of the parent compound at  $T_C = 95$  K, being in accord with its magnetic properties [20]. Partial substitution of U by Th lowers the Curie temperature down to about 29 K in  $\text{U}_{0.3}\text{Th}_{0.7}\text{NiSi}_2$  and the anomaly at  $T_C$  quickly evolves into a broad hump. In the alloy with  $x = 0.8$  only a weak and blurred anomaly can be found in the specific heat data at about 11 K.

Figure 5 displays the temperature variation of the increase of the magnetic entropy, defined as  $\Delta S(T) = \int_{T_{\min}}^T \frac{\Delta C}{T} dT$  (where  $T_{\min}$  stands for the low-temperature limit of the specific heat measurements). In  $\text{CeNiGe}_3$  (figure 5(a)),  $\Delta S$  at  $T_N$  is smaller than  $R \ln 2$  ( $\approx 5.76$  J/(mol K)), being the expected value for a disordered ground doublet. The reduction of the entropy is most probably due to the existence of short-range interactions above  $T_N$  (well visible as a characteristic tail in  $\Delta C(T)/T$  above  $T_N$ ; see figure 4(a)) and the Kondo effect (evidenced previously [13]). In  $\text{UNiSi}_2$  (figure 5(b)),  $\Delta S$  at  $T_C$  is much larger than  $R \ln 2$ , which points out at significant contribution of the excited crystalline electric field levels to the magnetic entropy at the ordering temperature.

In the paramagnetic region, the  $\Delta S(T)$  curves calculated for both the  $\text{Ce}_{1-x}\text{Y}_x\text{NiGe}_3$  (figure 5(a)) and  $\text{U}_{1-x}\text{Th}_x\text{NiSi}_2$  alloys (figure 5(b)) nearly superimpose onto each other, suggesting that the entropy contribution of the excited crystalline electric field levels is concentration independent in both systems studied. In other

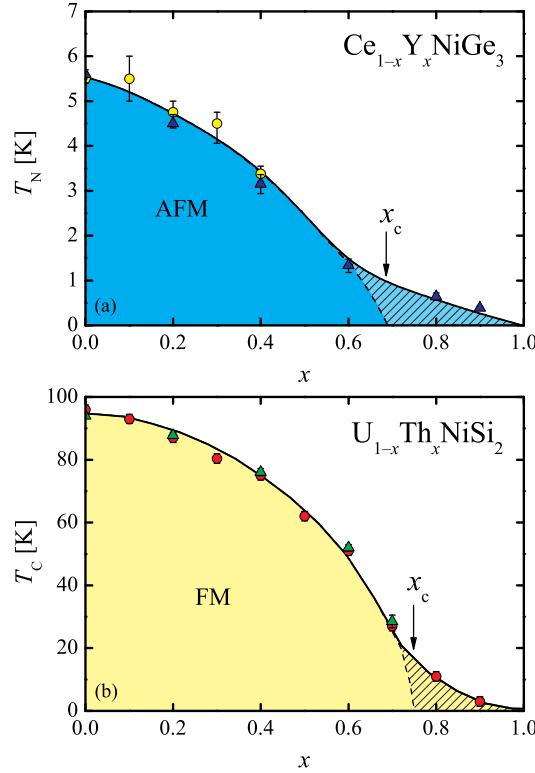


**Figure 6.** Tentative magnetic phase diagrams for  $\text{Ce}_{1-x}\text{Y}_x\text{NiGe}_3$  (a) and  $\text{U}_{1-x}\text{Th}_x\text{NiSi}_2$  (b). Circles correspond to the maxima in  $\chi(T)$  or to the minima in temperature derivative of  $\sigma(T)$ . Triangles represent the minimum in the temperature derivative of  $\Delta C(T)/T$ . Solid lines serve as guides for the eye and the arrows mark the critical concentrations.

words, the crystalline electric field in  $\text{Ce}_{1-x}\text{Y}_x\text{NiGe}_3$  and  $\text{U}_{1-x}\text{Th}_x\text{NiSi}_2$  is only weakly altered by the dilution of the magnetic sublattices, which is in line with the magnetic properties of the alloys. In the ordered region in turn, the temperature dependencies of the magnetic entropy of both systems strongly vary with  $x$ . In particular, upon increasing the Y/Th content up to  $x = 0.2$ , the kinks visible in  $\Delta S(T)$  of  $\text{CeNiGe}_3$  and  $\text{UNiSi}_2$  at the respective ordering temperatures move towards lower temperatures. For larger  $x$  the sharp anomalies at  $T_{N,C}$  evolve into broad, featureless curves.

#### 4. Discussion

Figure 6 displays tentative magnetic phase diagrams for the  $\text{Ce}_{1-x}\text{Y}_x\text{NiGe}_3$  and  $\text{U}_{1-x}\text{Th}_x\text{NiSi}_2$  alloys, constructed on the basis of the so-far obtained experimental data. The behaviour of both systems reminds those reported for diluted magnetic alloys [26]. In particular, in the Ce/U-rich part of the diagrams one can distinguish a dome of a long-range magnetic order, followed by a characteristic tail of a short-range magnetic order in the diluted limit. These two concentration regimes are separated from each other by the critical concentration  $x_c$ , roughly estimated by extrapolation of the initial slope of  $T_{N,C}(x)$  down to absolute zero temperature, as being of about 0.64 and 0.75 in



Ce<sub>1-x</sub>Y<sub>x</sub>NiGe<sub>3</sub> and U<sub>1-x</sub>Th<sub>x</sub>NiSi<sub>2</sub>, respectively.

The long-range character of the magnetic order of the alloys with  $x = 0.0$  and  $0.2$  can be deduced *i. a.* from the presence of pronounced anomalies in temperature dependencies of the magnetic entropy (figure 5). In particular, since the shape of  $\Delta S(T)$  is closely related to the magnetic structure and the thermal demagnetization processes, simple magnetic structures with high anisotropy yield sharp increase in the entropy with a distinct kink at the ordering temperature (cf. [27] and references therein). Upon rising  $x$ , an increasing degree of crystallographic disorder (introduced by the alloying) results in smearing the anomaly at  $T_{N,C}$  (figure 5). Finally, for large values of  $x$ , any kink in  $\Delta S(T)$  is hardly visible, although some weak anomalies are still visible in other physical characteristics studied (cf. figures 2, 3, 4). The latter fact, together with the change of the curvature in  $T_{N,C}(x)$  at  $x_c$  (figure 6), suggests a domination of short-range interactions at  $x > x_c$  (cf. [26]).

The observed evolution of the magnetic properties of the Ce<sub>1-x</sub>Y<sub>x</sub>NiGe<sub>3</sub> and U<sub>1-x</sub>Th<sub>x</sub>NiSi<sub>2</sub> alloys can be roughly explained as resulting from a nature of indirect-exchange Ruderman-Kittel-Kasuya-Yosida interactions, which are responsible for the onset of a magnetic order in metals. Since these interactions are a function of a distance between the localized magnetic moments, the random occupation of the Ce/Y and U/Th sites by the  $f$ -electrons leads most probably to an appearance in the most diluted alloys of magnetic clusters of different sizes and ordering temperatures [26]. As a consequence, the observed anomalies in the physical properties studied become more and more blurred with increasing  $x$ , and  $T_{N,C}$  represent a mean ordering temperature of the particular alloys. Since the size of the clusters remains finite far below the percolation threshold, a characteristic tail in the magnetic phase diagrams is visible (figure 6). The latter hypothesis need to be verified by further experiments, e.g. AC magnetic susceptibility, neutron diffraction etc.

## 5. Summary

The collected experimental data revealed that the dilution of the magnetic sublattices of CeNiGe<sub>3</sub> ( $T_N = 5.5$  K) and UNiSi<sub>2</sub> ( $T_C = 95$  K) leads to rapid decrease of their ordering temperatures down to about 1.35 K in Ce<sub>0.4</sub>Y<sub>0.6</sub>NiGe<sub>3</sub> and 29 K in U<sub>0.3</sub>Th<sub>0.7</sub>NiSi<sub>2</sub>. Further decrease of the Ce/U content results in the loss of the long-range character of the magnetic order at finite temperature and in formation of a characteristic tail in the magnetic phase diagrams. Therefore, no quantum critical phase transition can be observed in the systems studied. The observed evolution of the magnetic behaviour of the Ce<sub>1-x</sub>Y<sub>x</sub>NiGe<sub>3</sub> and U<sub>1-x</sub>Th<sub>x</sub>NiSi<sub>2</sub> is characteristic of the diluted magnetic alloys. Interestingly, the observed magnetic behaviour exhibits also some similarities to many solid solutions with fully occupied  $f$ -electron sublattices [28]. Further experiments are needed to clarify possible relationships between the latter systems and the two solid solutions studied.

## Acknowledgments

APP thanks D. Kaczorowski for helpful conversations. This work was supported by the Polish Ministry of Science and Higher Education within research grant no. N N202 102338.

## References

- [1] Stewart G R 2001 *Rev. Mod. Phys.* **73** 797
- [2] Stewart G R 2006 *Rev. Mod. Phys.* **78** 743
- [3] von Löhneysen H, Rosch A, Vojta M, Wölfle P 2007 *Rev. Mod. Phys.* **79** 1015
- [4] Miranda E, Dobrosavljević V 2005 *Rep. Prog. Phys.* **68** 2337
- [5] Pikul A P, Caroca-Canales N, Deppe M, Gegenwart P, Sereni J G, Geibel C, Steglich F 2006 *J. Phys.: Condens. Matter* **18** L535
- [6] Westerkamp T, Deppe M, Küchler R, Brando M, Geibel C, Gegenwart P, Pikul A P, Steglich F 2009 *Phys. Rev. Lett.* **102** 206404
- [7] Pikul A P, Geibel C, Oeschler N, Macovei M E, Caroca-Canales N, Steglich F 2010 *Phys. Status Solidi B* **247** 691
- [8] Pikul A P, Stockert U, Steppke A, Cichorek T, Hartmann S, Caroca-Canales N, Oeschler N, Brando M, Geibel C, Steglich F 2012 *Phys. Rev. Letters* **108** 066405
- [9] Pikul A P, Kaczorowski D 2011 *J. Phys.: Condens. Matter* **23** 456002
- [10] Pikul A P, Kaczorowski D 2011 *J. Phys. Soc. Jpn.* **80** SA107
- [11] Salamakha P, Konyk M, Sologub O, Bodak O 1996 *J. Alloys Compd.* **236** 206
- [12] Akselrud L G, Yarmolyuk Y P, Gladyshevskii E I 1979 *Visn. L'viv. Derzh. Univ., Ser. Khim.* **21** 18
- [13] Pikul A, Kaczorowski D, Plackowski T, Czopnik A, Michor H, Bauer E, Hilscher G, Rogl P, Grin Y 2003 *Phys. Rev. B* **67** 224417
- [14] Nakashima M, Tabata K, Thamizhavel A, Kobayashi T C, Hedo M, Uwatoko Y, Shimizu K, Settai R, Ōnuki Y 2004 *J. Phys.: Condens. Matter* **16** L255
- [15] Kotegawa H, Takeda K, Miyoshi T, Fukushima S, Hidaka H, Kobayashi T C, Akazawa T, Ohishi Y, Nakashima M, Thamizhavel A, Settai R, Ōnuki Y 2006 *J. Phys. Soc. Jpn.* **75** 044713
- [16] Harada A, Kawasaki S, Mukuda H, Kitaoka Y, Thamizhavel A, Okuda Y, Settai R, Ōnuki Y, Itoh K M, Haller E E, Harima H 2007 *J. Magn. Magn. Mater.* **310** 614
- [17] Harada A, Mukuda H, Kitaoka Y, Thamizhavel A, Okuda Y, Settai R, Ōnuki Y, Itoh K M, Haller E E, Harima H 2008 *Physica B* **403** 1020
- [18] Harada A, Mukuda H, Kitaoka Y, Thamizhavel A, Okuda Y, Settai R, Ōnuki Y, Itoh K M, Haller E E, Harima H 2008 *J. Phys. Soc. Jpn.* **77** 103710
- [19] Pikul A P, Gnida D 2011 *Solid State Commun.* **151** 778
- [20] Kaczorowski D 1996 *Solid State Commun.* **99** 949
- [21] Pikul A P, Kaczorowski D 2012 *Phys. Rev. B* **85** 045113
- [22] Sidorov V A, Tobash P H, Wang C, Scott B L, Park T, Bauer E D, Ronning F, Thompson J D, Fisk Z 2011 *J. Phys.: Conf. Series* **273** 012014
- [23] Pikul A, Kaczorowski D, Michor H, Rogl P, Bauer E, Hilscher G, Grin Y 2003 *J. Phys.: Condens. Matter* **15** 8837
- [24] Tateiwa N, Haga Y, Matsuda T D, Ikeda S, Nakashima M, Thamizhavel A, Settai R, Ōnuki Y 2006 *J. Phys. Soc. Jpn.* **75** Suppl. 174
- [25] Pikul A P, Kaczorowski D, Michor H, Rogl P, Czopnik A, Grin Y, Bauer E, Hilscher G 2003 *Acta Phys. Pol. B* **34** 1235
- [26] Mydosh J A, Spin glasses: an experimental introduction, Taylor & Francis, London–Washington, 1993

*The influence of magnetic sublattice dilution on magnetic order in  $CeNiGe_3$  and  $UNiSi_2$*

- [27] Marcano N, Espeso J I, Gómez Sal J C, Fernández J R, Herrero-Albillos J, Bartolomé F 2005  
*Phys. Rev. B* **71** 134401
- [28] Sereni J G 1998 *J. Phys. Soc. Jpn.* **67** 1767